Chinese Journal of Natural Medicines

Compatibility of cold herb CP and hot herb AZ in Huanglian Ganjiang decoction alleviates colitis mice through M1/M2 macrophage polarization balance *via* PDK4–mediated glucose metabolism reprogramming

Yanyang Li, Chang Liu, Yi Wang, Peiqi Chen, Shihua Xu, Yequn Wu, Lingzhi Ren, Yang Yu, Lei Yang

Citation: Yanyang Li, Chang Liu, Yi Wang, Peiqi Chen, Shihua Xu, Yequn Wu, Lingzhi Ren, Yang Yu, Lei Yang, Compatibility of cold herb CP and hot herb AZ in Huanglian Ganjiang decoction alleviates colitis mice through M1/M2 macrophage polarization balance *via* PDK4–mediated glucose metabolism reprogramming, Chinese Journal of Natural Medicines, 2025, 23(10), 1183–1194. doi: 10.1016/S1875–5364(25)60869–7.

View online: https://doi.org/10.1016/S1875–5364(25)60869–7

Chinese Journal of Natural Medicines 23 (2025) 1183-1194

Contents lists available at ScienceDirect

Chinese Journal of Natural Medicines

journal homepage: www.cjnmcpu.com/

Original article

Compatibility of cold herb CP and hot herb AZ in Huanglian Ganjiang decoction alleviates colitis mice through M1/M2 macrophage polarization balance *via* PDK4-mediated glucose metabolism reprogramming

Yanyang Li[a,Δ], Chang Liu[b,Δ], Yi Wang[a], Peiqi Chen[a], Shihua Xu[a], Yequn Wu[a], Lingzhi Ren[a], Yang Yu[a,*], Lei Yang[a,*]

[a] *School of Pharmaceutical Sciences, Guangzhou University of Chinese Medicine, Guangzhou 510006, China*

[b] *Guangdong Provincial Engineering Research Center for Quality and Safety of Traditional Chinese Medicine, Guangdong Provincial Key Laboratory of Chemical Measurement and Emergency Test Technology, Institute of Analysis, Guangdong Academy of Sciences (China National Analytical Center, Guangzhou), Guangzhou 510070, China*

ARTICLE INFO

Article history:
Received 3 September 2024
Revised 6 December 2024
Accepted 10 December 2024
Available online 20 October 2025

Keywords:
Compatibility
Colitis
Cold herb
Hot herb
Huanglian Ganjiang decoction
M1/M2 macrophage polarization
PDK4
Glucose metabolism reprogramming.

ABSTRACT

Ulcerative colitis (UC) is a chronic and non-specific inflammatory bowel disease (IBD). Huanglian Ganjiang decoction (HGD), derived from ancient book *Beiji Qianjin Yao Fang*, has demonstrated efficacy in treating UC patients traditionally. Previous research established that the compatibility of cold herb Coptidis Rhizoma + Phellodendri Chinensis Cortex (CP) and hot herb Angelicae Sinensis Radix + Zingiberis Rhizoma (AZ) in HGD synergistically improved colitis mice. This study investigated the compatibility mechanisms through which CP and AZ regulated inflammatory balance in colitis mice. The experimental colitis model was established by administering 3% dextran sulphate sodium (DSS) to mice for 7 days, followed by CP, AZ and CPAZ treatment for an additional 7 days. M1/M2 macrophage polarization levels, glucose metabolites levels and pyruvate dehydrogenase kinase 4 (PDK4) expression were analyzed using flow cytometry, Western blot, immunofluorescence and targeted glucose metabolomics. The findings indicated that CP inhibited M1 macrophage polarization, decreased inflammatory metabolites associated with tricarboxylic acid (TCA) cycle, and suppressed PDK4 expression and pyruvate dehydrogenase (PDH) (Ser-293) phosphorylation level. AZ enhanced M2 macrophage polarization, increased lactate axis metabolite lactate levels, and upregulated PDK4 expression and PDH (Ser-293) phosphorylation level. TCA cycle blocker AG-221 and adeno-associated virus (AAV)-PDK4 partially negated CP's inhibition of M1 macrophage polarization. Lactate axis antagonist oxamate and PDK4 inhibitor dichloroacetate (DCA) partially reduced AZ's activation of M2 macrophage polarization. In conclusion, the compatibility of CP and AZ synergistically alleviated colitis in mice through M1/M2 macrophage polarization balance *via* PDK4-mediated glucose metabolism reprogramming. Specifically, CP reduced M1 macrophage polarization by restoration of TCA cycle *via* PDK4 inhibition, while AZ increased M2 macrophage polarization through activation of PDK4/lactate axis.

1. Introduction

Ulcerative colitis (UC), a form of inflammatory bowel disease (IBD), manifests as continuous, superficial mucosal lesions originating in the rectum and extending to proximal segments of the colon [1]. The clinical manifestations of UC include diarrhea, haematochezia, abdominal pain, nausea and vomiting [2]. Although not fully elucidated, the pathogenesis of UC primarily involves genetics, environment, diet, immune response, microbiome and mucosal barrier function. Currently, several first-line treatments for UC, including 5-aminosalicylic acid, corticosteroids, biologics and thiopurines, demonstrate satisfactory clinical outcomes. However, extended use of individual medications results in various adverse effects, such as corticosteroid-induced osteoporosis, hypertension, and cataracts [3], as well as thiopurine-related acute pancreatitis and bone marrow suppression [4].

UC represents an autoimmune condition characterized by gut microbiota invasion of the colonic lamina propria, release of inflammatory mediators, and excessive immune response. The pathophysiological foundation of UC is inflammation, and inflammatory suppression proves effective for clinical remission. Macrophages, essential components of the innate immune system, quickly respond to immune microenvironment signals and differentiate into two distinct subtypes: classically activated (M1) and alternatively activated (M2) macrophages [5]. In response to lipopolysaccharide (LPS) and interferon-γ (IFN-γ), M0 macrophages develop an M1 phenotype. M1 macrophages express elevated levels of iNOS, cluster of differentiation 86 (CD86) and secrete pro-inflammatory cytokines TNF-α, interleukin-1β (IL-1β), IL-6

* Corresponding author.
E-mail addresses: yuyang@gzucm.edu.cn (Y. Yu); yanglei@gzucm.edu.cn (L. Yang)
Δ These authors contributed equally to this work.

https://doi.org/10.1016/S1875-5364(25)60869-7

to combat invading pathogens. Conversely, IL-4 and IL-13 stimulate M2 macrophage polarization. M2 macrophages express high levels of CD206, Arg-1 and produce IL-10 and TGF-β to resolve inflammation and repair tissue [6]. Research has shown that M1/M2 macrophage imbalance can trigger cytokine storms and sustained inflammatory responses, thereby exacerbating UC progression [7].

Glucose serves as the primary energy source supporting normal macrophage physiological functions through glycolysis and the tricarboxylic acid (TCA) cycle. In the cytoplasm, glycolysis metabolizes glucose into either pyruvate under aerobic conditions or lactate under anaerobic conditions. Aerobically produced pyruvate initiates the TCA cycle in mitochondria. Glucose metabolism plays a fundamental role in regulating M1/M2 macrophage polarization. M1 macrophages demonstrate enhanced glycolysis and TCA cycle inhibition to maintain proinflammatory functions and meet energy demands. In contrast, M2 macrophages maintain a complete TCA cycle chain and robust activity to generate sufficient ATP for mannose receptor glycosylation.

Pyruvate dehydrogenase (PDH) facilitates the metabolic conversion of pyruvate into acetyl-CoA *via* decarboxylation, contributing to initiation of TCA cycle. PDH activity is regulated by pyruvate dehydrogenase kinase 4 (PDK4), which belongs to PDK isozyme family members, through a reversible phosphorylation of 3 serine residues of the E1 α subunit on PDH (PDH1α): Ser232, Ser293 and Ser300 [8]. PDK4, one of the crucial isozyme family members, regulates glucose metabolism reprogramming and inflammatory response. PDK4 expression was elevated in dextran sulphate sodium (DSS)-induced colitis mice, while PDK4 inhibition improved colitis by regulating metabolic reprograming *via* mitochondria-associated membrane/calcium pathways in $CD4^+$ T cell, suggesting that PDK4 may be a potential treatment target for UC [9].

Traditional Chinese medicine (TCM) formula is composed of multiple TCM herbs based on the basic structure of "monarch, minister, adjuvant, guide" (Jun-Chen-Zuo-Shi). Huanglian Ganjiang decoction (HGD) was rooted in ancient book *Beiji Qianjin Yao Fang* written by Simiao Sun. HGD is composed of cold herb: Coptidis Rhizoma and Phellodendri Chinensis Cortex (CP); hot herb: Zingiberis Rhizoma and Angelicae Sinensis Radix (AZ); astringent herb: Sanguisorbae Radix and Asini Corii Colla. HGD was rooted from classic prescription Zhuche Pill and Wumei Pill, which had clinical therapeutic effect on UC patients [10, 11]. Traditionally, HGD has been prescribed for abdominal pain, tenesmus and haematochezia, which are in accordance with clinical manifestations of UC [12]. Additionally, Coptidis Rhizoma, a single herb of HGD, could reduce inflammatory response, enhance tight junction and restore gut flora structure in UC rats [13]. Our previous researches demonstrated that HGD displayed anti-colitis activity [14], as well as compatibility of CP and AZ regulated intestinal inflammation [15]. Meanwhile, chemical composition of CP, AZ, CPAZ water extracts were analyzed by UPLC-MS/MS in previous studies (Supplementary Fig. 1 and supplementary table 1) [15]. Nevertheless, the potential mechanism of compatibility of CP and AZ in alleviation of colitis mice remain obscure.

Hence, this study focused on the effects of compatibility of CP and AZ on glucose metabolism and M1/M2 macrophage polarization in colitis mice.

2. Materials and methods

2.1. Chemicals and reagents

Coptidis Rhizoma (Huanglian) (catalog No. 19110101), Phellodendri Chinensis Cortex (Huangbai) (catalog No. 19110201) were obtained from Jiangxi Zhangshu square Chinese Herbal Medicine Co., Ltd. Zingiberis Rhizoma (Ganjiang) (catalog No. 190901) was acquired from Guangzhou Nanbeihang Traditional Chinese Medicine Slices Co., Ltd. Angelicae Sinensis Radix (Danggui) (catalog No. 180802) was sourced from Anhui Jiquan Pharmaceutical Co., Ltd. Professor Guangtian Peng of Guangzhou University of Chinese Medicine authenticated these herbs (Fig. 1A). Voucher specimens were stored in herbarium C306 at the School of Pharmaceutical Sciences, Guangzhou University of Chinese Medicine, Guangzhou. CD86 antibody (catalog No. TD6332S), CD206 (catalog No. TD4149S), PDK4 (catalog No. TD7169S) were obtained from Abmart Shanghai Co., Ltd. DSS, clodronate liposomes (Clo-lip) (catalog No. 40337ES10), control liposomes (catalog No. 40338ES10) were acquired from Yeasen Biotechnology Co., Ltd. Sodium oxamate (catalog No. K405108) and sodium dichloroacetate (DCA) (catalog No. KM13368) were obtained from KKL Med Inc. Adeno-associated virus (AAV)-PDK4 was procured from Shanghai Genechem Co., Ltd. PDH activity kit (catalog No. BC0385) was acquired from Beijing Solarbio Science & Technology Co., Ltd.

2.2. CP, AZ and CPAZ preparation

CP, AZ and CPAZ water extracts were prepared according to previously established protocols [15]. AZ comprises 12 g Angelicae Sinensis Radix and 9 g Zingiberis Rhizoma , CP contains 6 g Coptidis Rhizoma and 12 g Phellodendri Chinensis Cortex, while CPAZ consists of both CP and AZ. The herbs were individually immersed in distilled water at a 1∶10 ratio, followed by reflux extraction (30 minutes per cycle, two cycles). The extracts were filtered through double-layered gauze, and the filtrates from both cycles were combined. The final filtrates were concentrated under reduced pressure to 132 mL.

2.3. DSS-caused experimental colitis mice establishment and treatment

Male C57BL/6 mice (6–8 weeks) were obtained from Guangdong Zhiyuan Biopharmaceutical Technology Co., Ltd. Animal use in this study was approved under ethics permit number SYXK (Yue) 2024-0202. The mice were housed in individually ventilated cages under standardized conditions (temperature: 20–24 °C; humidity: 53%–57%; 12 h light/dark cycle). This study adheres to the *Guide for the Care and Use of Laboratory Animals* published by the US National Institutes of Health (NIH publication No. 85-23, revised 1985).

The clinical human intake of Coptidis Rhizoma, Phellodendri Chinensis Cortex, Zingiberis Rhizoma and Angelicae Sinensis Radix in HGD are 6 g, 12 g, 9 g and 12 g crude herb/body/day, respectively. Using the body surface area normalization method and previous research [15], the administered doses of CP, AZ and CPAZ were converted from human to mouse as follows. CP: (6 g + 12 g) × 9.1 (scaling factor between human and mice) ÷ 60 kg (human body weight) ≈ 2.7 $g{\cdot}kg^{-1}$; AZ: (9 g + 12 g) × 9.1 ÷ 60 kg ≈ 3.2 $g{\cdot}kg^{-1}$; CPAZ: (6 g + 12 g + 9 g + 12g) × 9.1 ÷ 60 kg ≈ 5.9 $g{\cdot}kg^{-1}$.

For pharmacodynamic study, mice were randomly divided into 5 groups: control group, DSS group, CP group (2.7 $g{\cdot}kg^{-1}$), AZ group (3.2 $g{\cdot}kg^{-1}$) and CPAZ group (5.9 $g{\cdot}kg^{-1}$). Mice except those in the control group were exposed to 3% DSS in drinking water for 7 days to establish the colitis model. Subsequently, mice in 3 treatment groups were administered corresponding drugs by oral gavage for 7 days, while mice in control and DSS groups received purified water. Body weight changes, fecal characteristics, and fecal occult blood were monitored to evaluate disease activity index (DAI). On day 15, all mice were anesthetized by intraperitoneal injection of 1.25% avertin and euthanized, and thymus, spleens, colons, mesenteric lymph nodes, and blood were collected (Fig. 1B).

2.4. Histopathological analysis

Colons of mice were fixed in 4% paraformaldehyde, dehydrated, embedded in paraffin, sectioned in 4-μm sections and stained with hematoxylin and eosin (H&E). The colon sections were examined microscopically to evaluate the degree of histological damage as reported by Rath *et al.* [16].

2.5. *In vivo* intestinal macrophage deletion

In vivo intestinal macrophage deletion was conducted using Clo-lip as previously described [17, 18]. Mice were randomly divided into 5 groups: control group, DSS group, CPAZ group, CPAZ + Con-lip group and CPAZ + Clo-lip group. Clo-lip (200 μL, 5 mg·mL^{-1}) were administered intraperitoneally one day before DSS stimulation initiation, followed by injection every 2 days. Control mice received 200 μL control liposomes.

2.6. Pharmacologic inhibition of TCA cycle and lactate axis

All mice were randomly divided into 6 groups: control group, DSS group, CP group, AZ group, CP + AG-221 group and AZ + Oxamate group. For interruption of the TCA cycle, mice in the CP + AG-221 group received AG-221 (an antagonist of IDH2, 45 mg·kg^{-1}) and CP by oral gavage once daily for 7 days. For inhibition of the lactate axis, mice in the AZ + Oxamate group received intraperitoneal injections of oxamate (an antagonist of LDHA, 500 mg·kg^{-1}) and AZ by oral gavage once daily for 7 days.

2.7. Overexpression and pharmacologic inhibition of PDK4

All mice were randomly divided into 6 groups: control group, DSS group, CP group, AZ group, CP + AAV-PDK4 group and AZ + DCA group. To establish PDK4 overexpression mice, subjects in the CP + OE-PDK4 group received intraperitoneal injections of AAV-PDK4 (5×10^{11} v. g/per mouse) 2 weeks prior to colitis induction and administration. Subsequently, all mice except the control group were challenged with DSS and treated with corresponding drugs. DCA served as a PDK4 inhibitor. In the AZ + DCA group, mice received oral administration of AZ and intraperitoneal injections of DCA (100 mg·kg^{-1}) once daily for 7 days after colitis induction.

2.8. Western blot

Protein samples underwent separation through SDS-polyacrylamide gel electrophoresis before transfer to PVDF membranes. The membranes were blocked using FastBlock Blocking Buffer for 15 min, followed by overnight incubation with primary antibodies at 4 °C. The following day, the membranes were incubated with HRP-conjugated secondary antibody for 1 h. The protein bands were then visualized using the chemiluminescence imaging system.

2.9. PDH activity assay

0.1 g of colon tissue was weighed, homogenized and centrifuged (4 °C, 11 000 × *g*, 10 min), and the supernatant was collected for subsequent analysis. Subsequently, 180 μL 2,6-dichloroindopheno and 10 μL distilled water were combined in the 96-well plate, followed by measurement of absorbance values at 10 sec (A1) and 1 min 10 sec (A2) at 605 nm. Similarly, 180 μL 2,6-dichloroindopheno and 10 μL supernatant sample were combined in the 96-well plate, followed by measurement of absorbance values at 10 sec (A3) and 1 min 10 sec (A4) at 605 nm. The PDH activity was calculated using the following formula.

$\Delta A_{\text{blank}} = A_1 - A_2$; $\Delta A_{\text{measurement}} = A_3 - A_4$; PDH activity (U·g^{-1}) = 1827.62 × ($\Delta A_{\text{measurement}} - \Delta A_{\text{blank}}$) ÷ colon sample weight.

2.10. Immunofluorescence

Paraffin sections of colon were deparaffinized with xylene and dehydrated with pure ethanol, followed by antigen retrieval with EDTA antigen retrieval solution. The tissue was circumscribed with a Liquid Blocker PAP Pen and blocked with 10% donkey serum for 30 min. Subsequently, sections were incubated with anti-F4/80, anti-CD86, anti-CD206 primary antibodies at 4 °C overnight. The corresponding secondary antibodies were incubated at room temperature for 50 min in darkness. The sections were washed with PBS three times and nuclei were stained with DAPI for 10 min in darkness. Fluorescence signals were observed using a laser scanning confocal microscope.

2.11. Flow cytometry

Mesenteric lymph nodes were harvested and processed into single-cell suspensions. The cells were labeled with surface marker antibody PE anti-F4/80 at room temperature for 30 min, followed by permeabilization. Subsequently, the suspensions were stained with intracellular antibodies PE-cy7 anti-CD86 and APC anti-CD206 for 30 min. Fluorescence signals were analyzed using a flow cytometer.

2.12. Targeted glucose metabolomics

Fecal samples (80 mg) were homogenized with 100 μL distilled water. The homogenate was combined with 400 μL methanol/acetonitrile solution, sonicated, centrifuged, and the supernatant was collected.

The supernatant samples were separated using Agilent 1290 Infinity LC. The conditions were as follows: mobile phase A: 50 mmol·L^{-1} ammonium acetate solution with 1.2% ammonium hydroxide; mobile phase B: 1% diacetone in acetonitrile solution; flow rate: 300 μL·min^{-1}; injection volume: 2 μL. The multi-step linear elution gradient program was: 1–10 min, 70%–60% B; 10–12 min, 60–30% B; 12.1–15 min, 30% B.

Mass spectrometry analysis was performed using a 5500 QTRAP mass spectrometer. In ESI negative modes, the parameters were set as follows: source temperature: 450 °C; Ion Source Gas1: 45 psi; Ion Source Gas2: 45 psi; Curtain gas: 30 psi; Ion Spray Voltage Floating: −4500 V.

Isotope internal standard quantitation was employed for quantitative analysis. The absolute contents of metabolites were calculated using the response abundance ratio (peak area ratio) between metabolites and internal standard, combined with the known concentration of internal standard. The quantitative procedure was as follows: First, the standard curve equation was derived from the mass spectrum signal information of the standard substance at different concentrations. Then, metabolite concentrations in the fecal sample were calculated using the standard curve. Finally, the metabolite contents were calculated based on the initial mass of fecal sample. The quantitative formula is presented below.

The content of metabolites in the fecal sample (μmol·g^{-1}) = $c \times V/\text{m} \times \text{n}$.

c: the concentration of metabolite calculated according to the standard curve.

V: the volume corresponding to standard curve point.

m: the weight of fecal sample.

n: dilution factor.

2.13. Statistical analysis

Statistical analysis was performed using GraphPad Prism 8.3 software. Dunnett's T3 tests were employed for comparisons among groups with heterogeneous variance, while Tukey's tests were utilized for groups with homogeneous variance. Statistical significance was defined as $P < 0.05$.

3. Results

3.1. CP, AZ and CPAZ attenuated DSS-caused colitis associated symptoms

To evaluate the therapeutic effects of CP, AZ and CPAZ on colitis development, mice were challenged with DSS for 7 days followed by drug treatment for an additional 7 days. Compared to the DSS group, administration of CP, AZ and CPAZ reduced weight loss, lowered DAI scores, increased thymus index, decreased spleen index, and restored colon length, with CPAZ demonstrating superior efficacy (Figs. 1C–1G). Histological analysis indicated that CP, AZ and CPAZ ameliorated DSS-induced colonic tissue damage, including epithelial cell exfoliation, inflammatory cell infiltration in mucosa and submucosa layers, mucos-

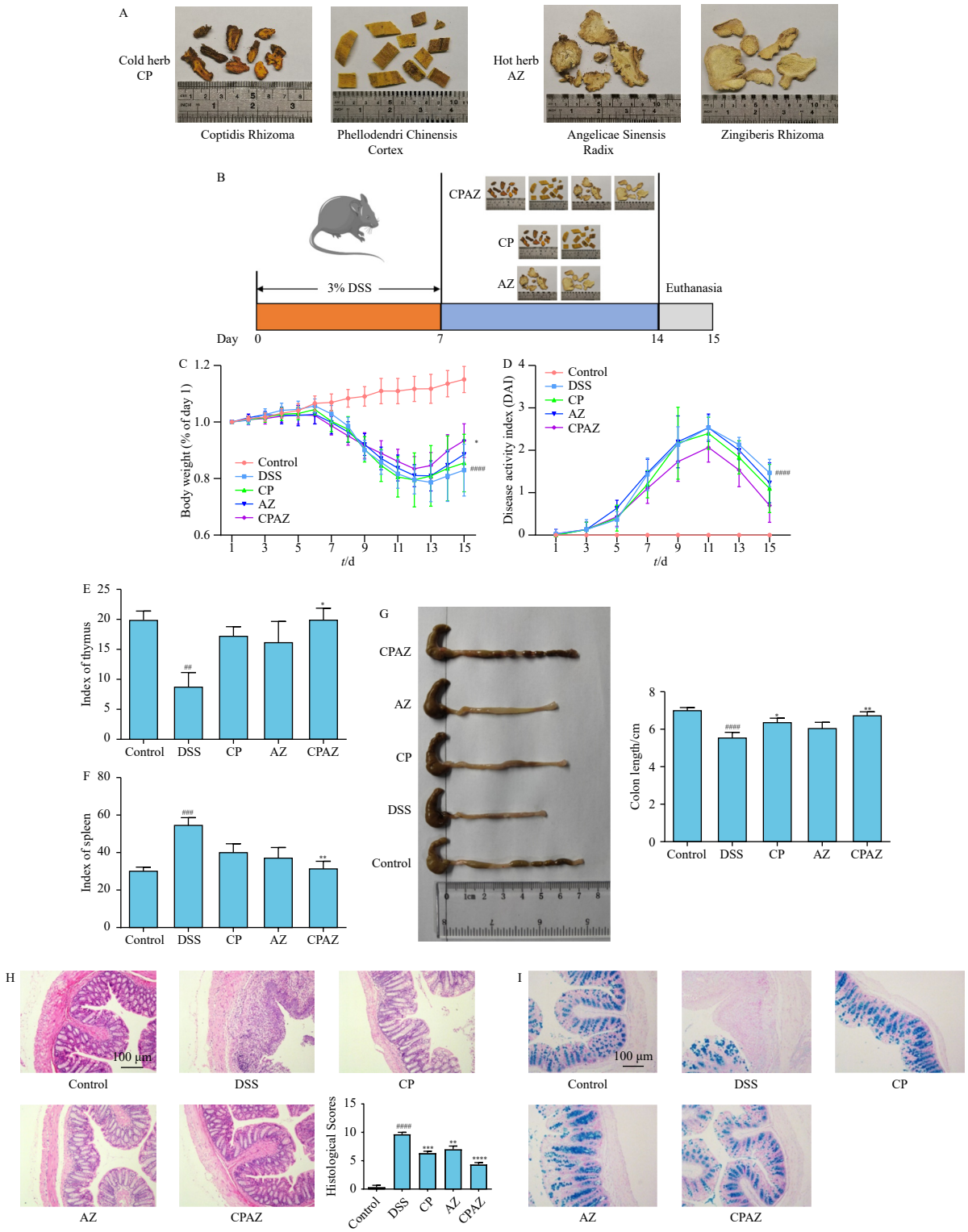

Fig. 1 CP, AZ and CPAZ attenuated DSS-caused colitis associated symptoms. (A) Composition of herbs in CP and AZ. (B) Flow chart of colitis mice model construction and drug intervention. (C) Body weight loss and recovery. (D) DAI score changes. (E) Index of thymus. (F) Index of spleen. (G) Macroscopical structures and lengths of colons. (H) Histopathological observation of colons by H&E staining (100 ×). (I) Histopathological observation of colons by alcian blue staining (100 ×). The results were expressed as mean ± SD (n = 6). $^{\#\#}P < 0.01$, $^{\#\#\#}P < 0.001$, $^{\#\#\#\#}P < 0.0001$ *vs* control group; $^{*}P < 0.05$, $^{**}P < 0.01$, $^{***}P < 0.001$, $^{****}P < 0.0001$ *vs* DSS group.

al edema, and goblet cell depletion (Figs. 1H–1I).

3.2. CP, AZ and CPAZ regulated M1/M2 macrophage polarization in colitis mice

The effects of CP, AZ and CPAZ on M1/M2 macrophage polarization were assessed using flow cytometry, Western blot, and immunofluorescence analyses. DSS challenge resulted in elevated levels of M1 macrophages ($F4/80^+$ $CD86^+$) and reduced levels of M2 macrophages ($F4/80^+$ $CD206^+$). CP and AZ exhibited distinct effects on CD86 and CD206 expression. Specifically, CP significantly reduced M1 macrophages, while AZ significantly increased M2 macrophages. CPAZ treatment demonstrated both a significant reduction in M1 macrophages and enhancement of M2 macrophages (Figs. 2A–2E).

3.3. Macrophages were essential for CPAZ-mediated therapeutic effect in colitis mice

To determine whether macrophages mediate the therapeutic effect of CPAZ, intestinal macrophages were depleted using Clo-lip, followed by colitis induction and drug intervention (Fig. 3A). The CPAZ + Clo-lip group exhibited significantly reduced intestinal macrophages compared to the CPAZ + Con-lip group, confirming successful macrophage depletion (Fig. 3B). Furthermore, the CPAZ + Clo-lip group demonstrated marked body weight loss, elevated DAI, decreased thymus index ($P < 0.05$) and colon length ($P < 0.05$), and increased histological score ($P < 0.05$) compared to the CPAZ + Con-lip group (Figs. 3C–3I). These findings suggest that macrophages may serve as key cellular mediators of CPAZ's protective effects in colitis mice.

3.4. CP, AZ and CPAZ adjusted glucose metabolism reprogramming in colitis mice

Compared with the control group, levels of lactate ($P < 0.001$) and α-ketoglutarate ($P < 0.05$) were significantly decreased, while the levels of pyruvate ($P < 0.05$), succinate, L-malic acid ($P < 0.05$), fumarate, and citrate were elevated (Figs. 4A–4G). CP demonstrated a decreasing trend in TCA cycle inflammatory metabolites, including citrate, L-malic acid, succinate, and fumarate contents in colitis mice, primarily implicated in M1 macrophage polarization, though without significant differences. AZ significantly increased the lactate axis metabolite content ($P <$

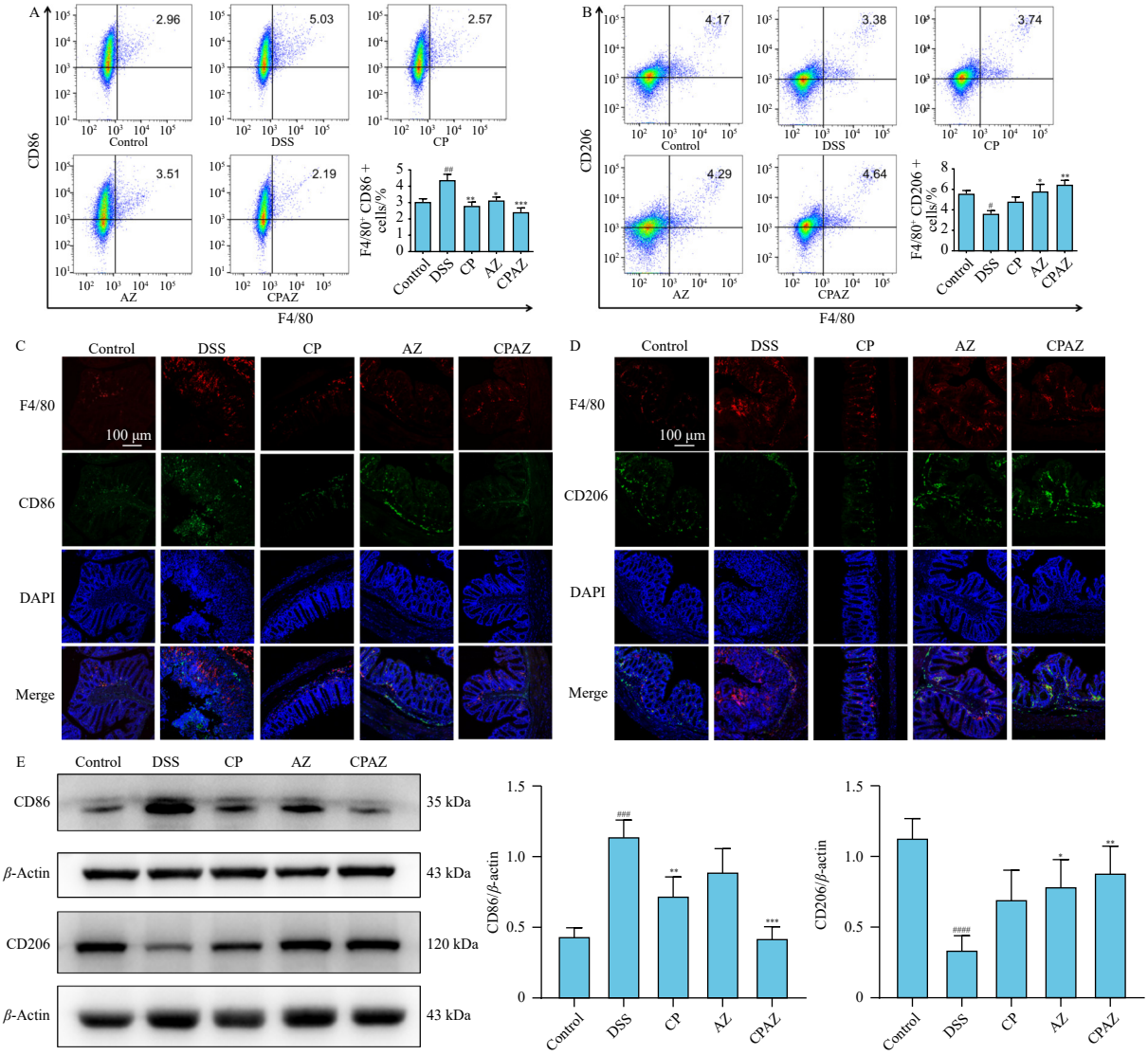

Fig. 2 CP, AZ and CPAZ regulated M1/M2 macrophage polarization in colitis mice. (A) Flow cytometry analysis of M1 macrophage ($F4/80^+$ $CD86^+$) cells. (B) Flow cytometry analysis of M2 macrophage ($F4/80^+CD206^+$) cells . (C) Immunofluorescence analysis of M1 macrophage cells in colon. (D) Immunofluorescence analysis of M2 macrophage cells in colon. (E) Western blot analysis of CD86 and CD206 expressions. The results were expressed as mean ± SD ($n = 6$). $^{\#\#}P < 0.01$, $^{\#\#\#}P < 0.001$ *vs* control group. $^{*}P < 0.05$, $^{**}P < 0.01$, $^{***}P < 0.001$, $^{****}P < 0.0001$ *vs* DSS group.

0.01) in colitis mice, closely associated with M2 macrophage polarization. Additionally, mice treated with CPAZ showed a reduction trend in citrate, L-malic acid, succinate, and fumarate levels, while exhibiting an elevated trend in lactate and α-ketoglutarate levels, though differences were not significant. These findings suggest that CP might enhance TCA cycle activity, AZ might promote the lactate axis, and CPAZ might strengthen both pathways in colitis mice.

3.5. The effects of CP and AZ on M1/M2 macrophage polarization were depended on glucose metabolism

To further investigate the role of glucose metabolism in CP and AZ-treated colitis mice, TCA cycle blocker AG-221 and lactate axis inhibitor oxamate were employed (Fig. 5A). Oxamate decreased lactate production by inhibiting lactate dehydrogenase activity. AG-221 disrupted the TCA cycle by selectively inhibiting isocitrate dehydrogenase 2 (IDH2), which catalyzes the conversion of isocitrate to α-ketoglutarate [19]. As expected, mice co-administered with AZ and oxamate showed increased susceptibility to DSS-induced colitis, evidenced by higher spleen index, lower thymus index, reduced colon length, more severe histopathological structural damage, and decreased CD206 expression compared to the AZ group. In the CP + AG-221 group, mice exhibited greater colon length reduction, lower thymus index, higher spleen index, more extensive epithelial cell loss, increased inflammatory cell infiltration, and enhanced CD86 expression compared to CP-treated mice (Figs. 5B–5G). These observations confirmed glucose metabolism's essential role in M1/M2 macrophage polarization and the therapeutic effects of CP and AZ on colitis mice.

3.6. CP, AZ and CPAZ modified PDK4/p-PDH expression in colitis mice

PDK4 specifically phosphorylates Ser293-PDHE1α and inactivates PDH [8], thus p-Ser293-PDH levels were measured to assess PDK4 expression changes. Western blot analysis revealed that compared to the control group, PDK4 and downstream PDH (Ser-293) phosphorylation levels were significantly elevated in the DSS group ($P < 0.05$, $P < 0.01$). CP, AZ, and CPAZ differently modulated PDK4 and downstream PDH (Ser-293) phosphorylation levels. CP significantly reduced PDK4 and downstream p-Ser293-PDH levels ($P < 0.0001$, $P < 0.001$), while AZ increased PDK4 and downstream p-Ser293-PDH/PDH levels ($P < 0.05$). CPAZ markedly decreased PDK4 and downstream p-Ser293-PDH/PDH levels ($P < 0.05$, $P < 0.01$), though slightly less effectively than CP. PDH expression showed no significant changes across all groups (Figs. 6A–6B). Consistent with Western blot results, immunofluorescence analysis revealed increased PDK4 expression in the AZ group and decreased PDK4 expression in the CP and CPAZ groups compared to the DSS group (Fig. 6C). Additionally, PDH activity assessment showed reduced activity in the CP ($P < 0.01$) and CPAZ groups ($P < 0.05$), particularly in the CP group, while activity was elevated in the AZ group compared to the DSS group (Fig. 6D).

3.7. PDK4 was crucial for macrophage polarization regulation and anti-colitis effect of CP and AZ

To examine whether the intestinal protective effects of CP and AZ were mediated through PDK4, mice received PDK4 inhibitor DCA with AZ in the AZ + DCA group, while mice in the CP + AAV-PDK4 group were injected with AAV-PDK4 and treated with CP (Fig. 7A). In the AZ + DCA group, DCA partially reversed the therapeutic effect and M2 macrophage upregulation of AZ in colitis mice, evidenced by increased spleen index, reduced thymus index and colon length, significant histopathological structural damage, and decreased CD206 expression (Figs. 7B–7G). Additionally, intraperitoneal injection of AAV-PDK4 partially counteracted the intestinal protective effect and M1 macrophage downregulation of CP in colitis mice, as demonstrated by

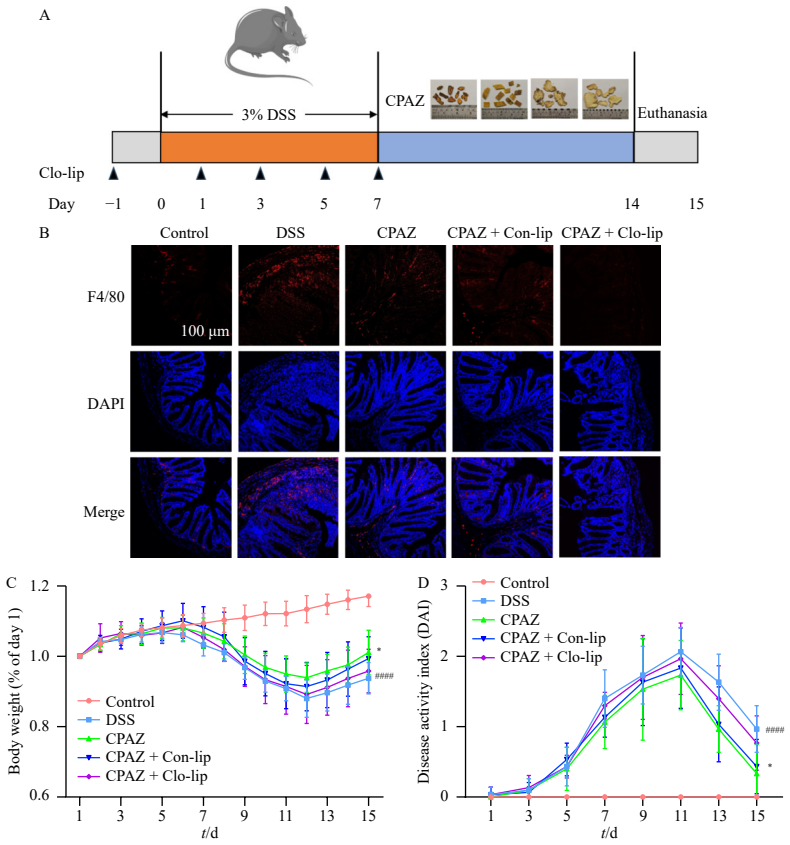

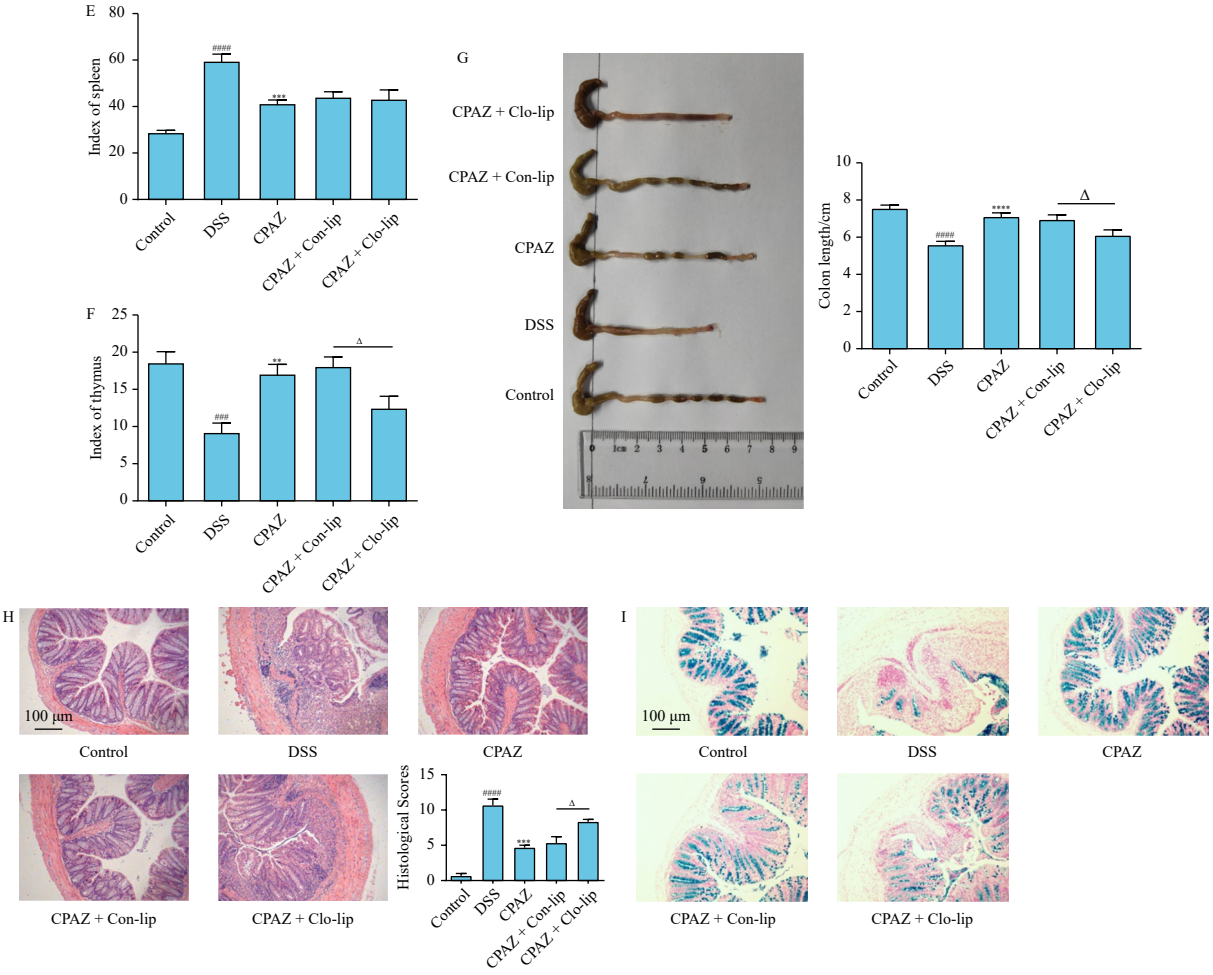

Fig. 3 Macrophages were essential for CPAZ-mediated therapeutic effect in colitis mice. (A) Establishment of macrophage deletion model construction and drug intervention. (B) Immunofluorescence analysis of macrophages (F4/80$^+$). (C) Body weight loss and recovery. (D) DAI score changes. (E) Index of spleen. (F) Index of thymus. (G) Macroscopical structures and lengths of colons. (H) Colon histopathological observation by H&E staining (100 ×). (I) Colon histopathological observation of colons by alcian blue staining (100 ×). The results were expressed as mean ± SD (n = 6). $^{###}P < 0.001$, $^{####}P < 0.0001$ *vs* control group. $^{*}P < 0.05$, $^{**}P < 0.01$, $^{***}P < 0.001$, $^{****}P < 0.0001$ *vs* DSS group. $^{\triangle}P < 0.05$ *vs* CPAZ + Clo-lip group.

elevated spleen index, reduced thymus index and colon length, limited histological improvement, and increased CD86 expression (Figs. 7B–7G). These findings aligned with Western blot results. Intraperitoneal injection of AAV-PDK4 significantly elevated PDK4 expression compared to the AAV-NC group, confirming successful establishment of the PDK4 overexpression mouse model (Supplementary Fig. 2). DCA plus AZ significantly reduced p-Ser293-PDH expression compared to the AZ group ($P < 0.0001$). AAV-PDK4 plus CP substantially increased p-Ser293-PDH / PDH levels compared to the CP group ($P < 0.0001$) (Fig. 7H). These data indicated that PDK4 was essential for M1/M2 macrophage polarization regulation and the anti-colitis effects of CP and AZ.

4. Discussion

UC represents an intestinal inflammatory condition characterized by recurring inflammation and extensive tissue damage. As UC involves interactions among multiple biological systems, achieving satisfactory clinical outcomes with monotherapy remains challenging. Current UC treatment emphasizes "cocktail" therapy, combining multiple drugs to achieve high cure rates and low recurrence rates [20], similar to TCM formula compatibility. TCM formulas combine multiple herbs according to their properties and compatibility theories, such as Monarch-Minister-Adjuvant-Guide (Jun-Chen-Zuo-Shi), rather than simply aggregating various TCM herbs [21]. This multi-component and multi-target approach delivers comprehensive therapeutic effects with minimal adverse reactions, aligning with UC treatment strategies. Understanding TCM compatibility mechanisms remains essential for clinical guidance, despite challenges posed by the complex nature of TCM formulas [22]. Previous research demonstrated that CP and AZ compatibility exhibited synergistic effects in treating colitis mice [15]. This study aims to elucidate the compatibility mechanisms through which CP and AZ regulate inflammatory balance.

To evaluate CP, AZ and CPAZ effects on colitis development, mice were challenged with 3% DSS and received drug treatments. CP, AZ and CPAZ demonstrated colitis attenuation, characterized by accelerated weight recovery post-DSS withdrawal, reduced colon shrinkage, decreased DAI score and spleen index, and significant histological improvement in the colon. These pharmacodynamic data indicated that CP and AZ compatibility synergistically improved the condition of colitis mice.

Macrophages, the predominant leukocyte population in the intestine, demonstrate significant plasticity in their M1/M2 differentiation, potentially explaining their diverse roles in UC development. During the initial phase of UC, M1 macrophages eliminate pathogens and trigger adaptive immune responses through pro-inflammatory mechanisms. Subsequently, M2 macrophages increase anti-inflammatory mediators to repair intestinal damage caused by M1 macrophages. Disruption of M1/M2 polarization balance in UC leads to chronic inflammation [23]. To investigate the effects of CP, AZ, and CPAZ on macrophages, analyses using Western blot, flow cytometry, and immunofluorescence were performed. The results indicated that CP primarily inhibited M1

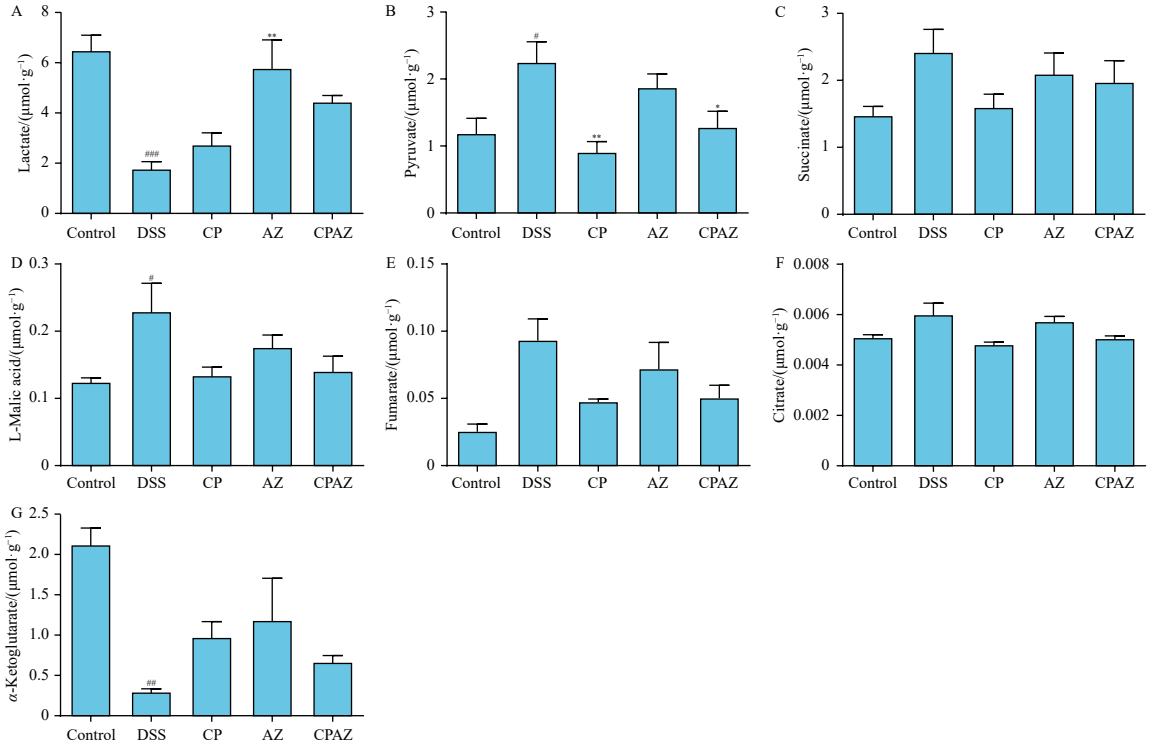

Fig. 4 CP, AZ and CPAZ adjusted glucose metabolism reprogramming in colitis mice. Contents of (A) Lactate. (B) Pyruvate. (C) Succinate. (D) L-malic acid. (E) Fmuarate. (F) Citrate. (G) *α*-Ketoglutarate. The results were expressed as mean ± SD (n = 6). $^{\#}P < 0.05$, $^{\#\#}P < 0.01$, $^{\#\#\#}P < 0.001$ *vs* control group; $^{*}P < 0.05$, $^{**}P < 0.01$ *vs* DSS group.

macrophage polarization, AZ predominantly enhanced M2 macrophage polarization, while CPAZ accomplished both effects. These findings demonstrate that individual administration of CP or AZ showed limited impact on macrophage polarization, whereas their combination effectively regulated M1/M2 macrophage balance in colitis mice.

Additionally, intestinal macrophage deletion mice were developed to examine the relationship between macrophages and CPAZ effects on colitis mice. Pharmacodynamic analysis revealed that CPAZ could impede colitis progression; however, macrophage depletion partially negated CPAZ's anti-colitis effects, indicating macrophages' significant role in CPAZ-treated colitis mice. This observation raised questions about the mechanisms through which CP, AZ, and CPAZ modulate macrophage polarization.

During UC, metabolic reprogramming occurs in activated M1 cells to facilitate cytokine production and immune responses [24]. The TCA cycle experiences two enzymatic breaks in M1 macrophages [25]. The first break, mediated by IDH, results in citrate accumulation and *α*-ketoglutarate deficiency. Citrate contributes to inflammatory mediator synthesis, including prostaglandin E2 (PGE2) and NO, through mitochondrial TCA cycle extraction *via*

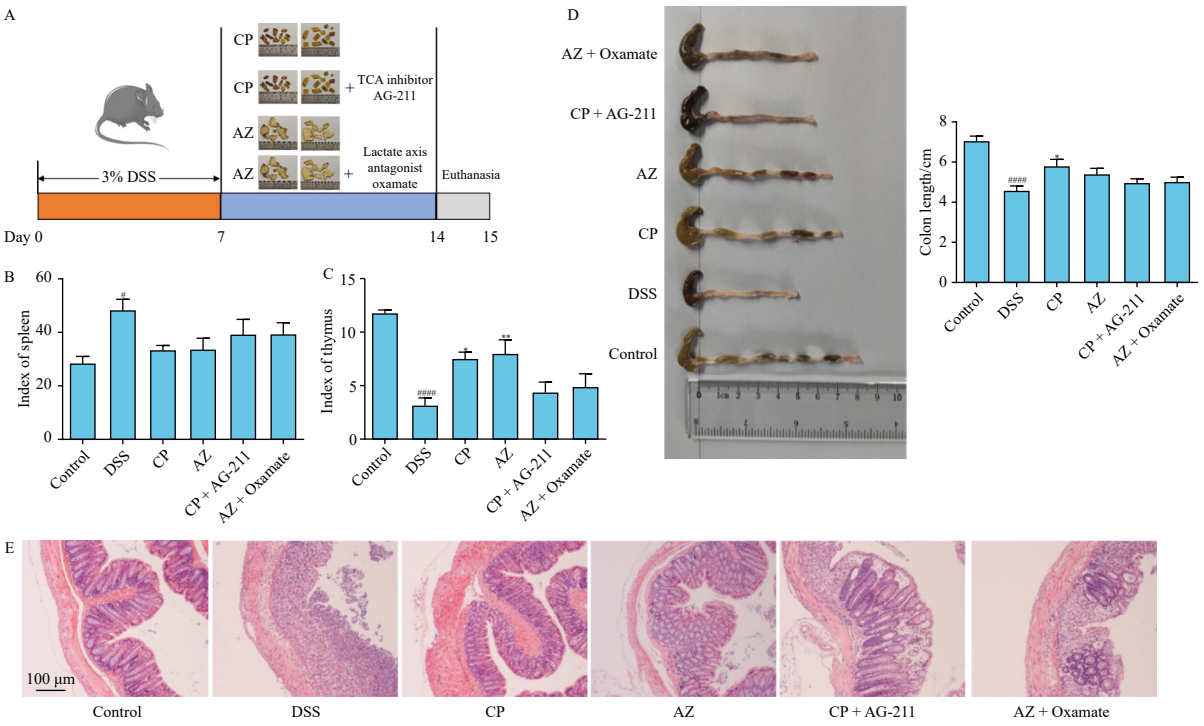

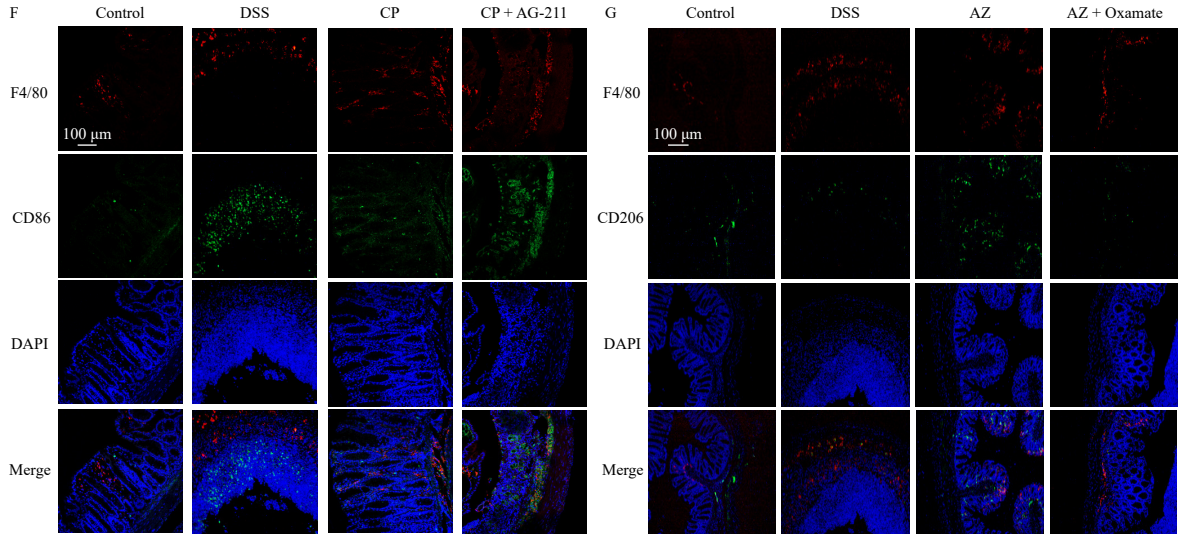

Fig. 5 The effects of CP and AZ on M1/M2 macrophage polarization were depended on glucose metabolism. (A) Construction of colitis model as well as pharmacologic inhibition of TCA cycle and lactate axis. (B) Index of spleen. (C) Index of thymus . (D) Macroscopical structures and lengths of colons. (E) Histopathological observation of colons by H&E staining (100 ×). (F) Immunofluorescence analysis of M1 (F4/80$^+$ CD86$^+$) cells in colon. (G) Immunofluorescence analysis of M2 (F4/80$^+$ CD206$^+$) cells in colon. The results were expressed as mean ± SD (n = 6). $^{\#}P < 0.05$, $^{\#\#\#}P < 0.001$, $^{\#\#\#\#}P < 0.0001$ *vs* control group. $^{*}P < 0.05$, $^{**}P < 0.01$, $^{***}P < 0.001$, $^{****}P < 0.000\ 1$ *vs* DSS group.

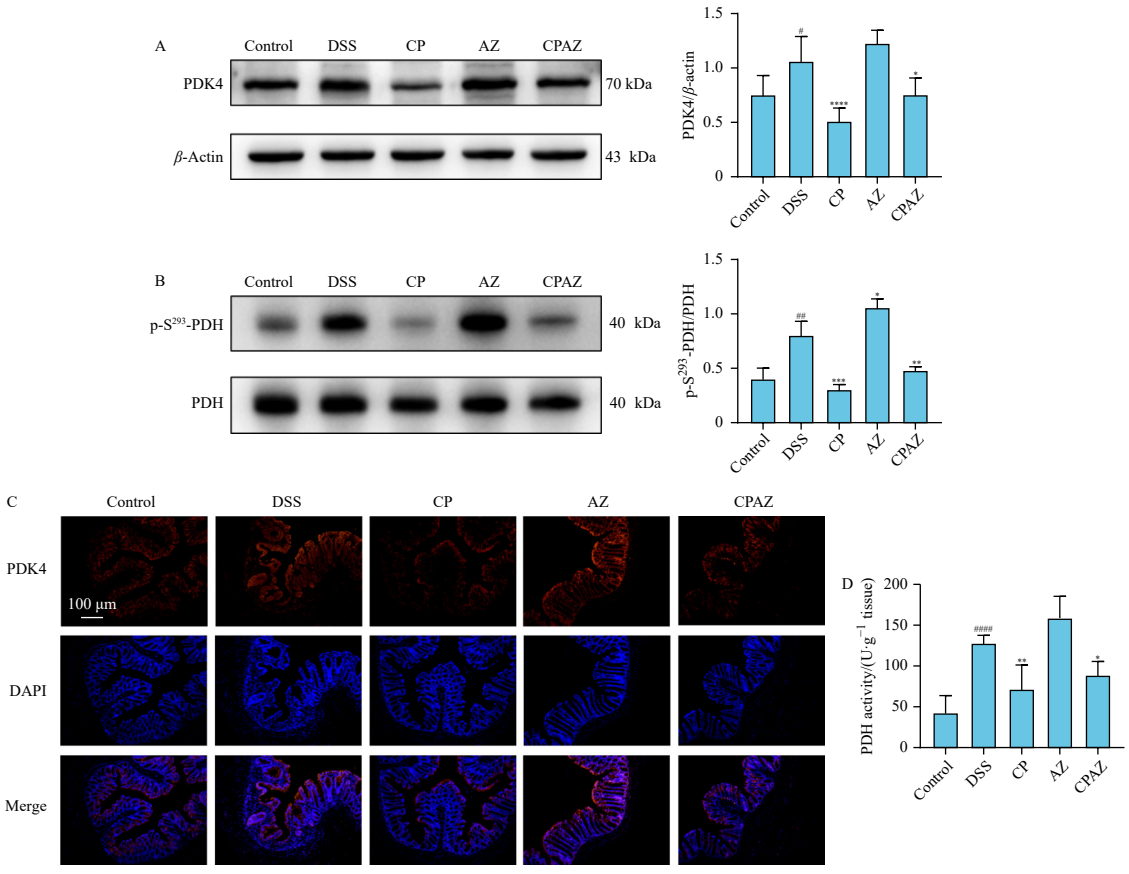

Fig. 6 CP, AZ and CPAZ modified PDK4/p-PDH expression in colitis mice. Western blot analysis of (A) PDK4. (B) p-S293-PDH. (C) immunofluorescence analysis of PDK4 (100 ×). (E) Activity of PDK4 . The results were expressed as mean ± SD (n = 6). $^{\#}P < 0.05$, $^{\#\#}P < 0.01$, $^{\#\#\#\#}P < 0.0001$ *vs* control group. $^{*}P < 0.05$, $^{**}P < 0.01$, $^{***}P < 0.001$, $^{****}P < 0.0001$ *vs* DSS group.

citrate carrier (CIC) [26-28]. α-Ketoglutarate promotes M2 macrophage polarization through Jmjd3-mediated epigenetic modification and fatty acid oxidation (FAO) enhancement, while limiting M1 macrophage activation by IKKβ inhibition [29]. The second break, controlled by succinate dehydrogenase, leads to succinate accumulation. Succinate induces pyruvate kinase M2 (PKM2) lysine succinylation, enabling nuclear translocation and HIF-1α interaction, promoting IL-1β release [30, 31]. Glucose metabolism analysis showed that CP and CPAZ decreased inflammatory TCA cycle metabolites, explaining their inhibitory effect on M1 macrophage polarization.

When TCA cycle disruption occurs, accumulated pyruvate converts to lactate *via* LDH. Recent evidence indicates that lactate, beyond its role as a glycolysis byproduct, serves an immunoregulatory function [32]. Lactate promotes M2 macrophage polarization through multiple pathways, including ERK/STAT3 [33],

PI3K/Akt [34], mTORC1/ATP6V0d2/HIF-2α [35], G-protein-coupled-receptor (GPR)/cAMP/CREM signaling [36], and histone lactylation [37, 38]. Additionally, lactate inhibits TLR4/NF-kB pathway activation and pro-inflammatory factor release, protecting against DSS-induced gut barrier injury [39]. However, excessive lactate accumulation can cause adverse effects, including acidosis, immunosuppression, and tumor progression [40, 41]. Therefore, metabolic intervention may regulate M1/M2 macrophage polarization and resolve intestinal inflammation [42]. Glucose metabolism analysis revealed elevated lactate levels with AZ and CPAZ treatment, explaining their M2 macrophage polarization effects.

Furthermore, TCA cycle blocker AG-221 and lactate axis inhibitor oxamate were employed to establish connections between glucose metabolism reprogramming and macrophage alterations

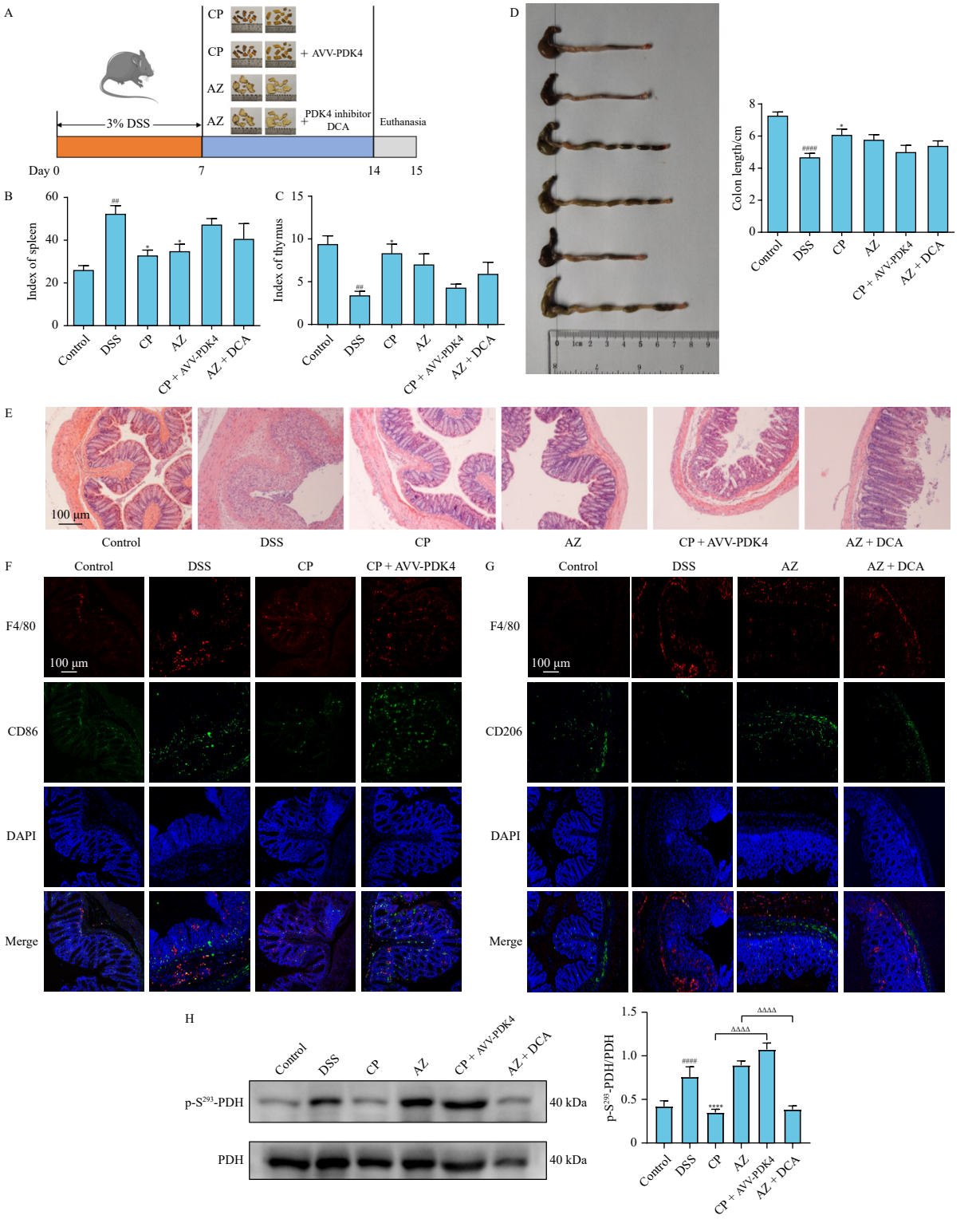

Fig. 7 PDK4 was crucial for macrophage polarization regulation and anti-colitis effect of CP and AZ. (A) Construction of colitis model as well as overexpression and pharmacologic inhibition of PDK4. (B) Index of spleen. (C) Index of thymus. (D) Macroscopical structures and lengths of colons. (E) Macroscopical structures and lengths of colons (100 ×). (F) Immunofluorescence analysis of M1 (F4/80$^+$ CD86$^+$) cells in colon. (G) Immunofluorescence analysis of M2 (F4/80$^+$ CD206$^+$) cells in colon. (H) Western blot of p-S293-PDH expression. DCA, Sodium dichloroacetate. The results were expressed as mean ± SD (n = 6). $^{\#\#}P < 0.01$, $^{\#\#\#\#}P < 0.0001$ *vs* control group. $^{*}P < 0.05$, $^{****}P < 0.0001$ *vs* DSS group. $^{\triangle\triangle\triangle\triangle}P < 0.0001$ *vs* CP & AZ group.

induced by CP and AZ. Notably, oxamate partially counteracted AZ-induced M2 macrophage polarization and anti-colitis effects, indicating lactate axis involvement in AZ-mediated M2 macrophage activation and colitis attenuation. AG-221 partially reversed CP-induced M1 macrophage suppression and colitis improvement, suggesting CP's mechanism involves TCA cycle regulation. However, the upstream mechanisms through which CP and AZ regulate glucose metabolism-mediated macrophage polarization remain unclear.

PDK4, a member of the PDK isozyme family, functions as a crucial enzyme regulating glucose metabolism in macrophages. PDK4 specifically phosphorylates Ser293-PDHE1α and inactivates PDH [8], inhibiting the conversion of pyruvate to acetyl-coA, which disrupts the TCA cycle and enhances glycolysis [43]. When PDK4 expression increases, the disrupted TCA cycle leads to an accumulation of pro-inflammatory TCA intermediates, including citrate, succinate, and fumarate. Our findings revealed that CP exhibited reduced levels of PDH activity, PDK4, and downstream p-PDH/PDH expressions, suggesting that CP might decrease PDK4 expression to restore the TCA cycle and suppress M1 macrophage polarization. Additionally, sustained PDK4 overactivation redirects pyruvate conversion from acetyl-CoA toward lactic acid, thereby increasing intracellular lactic acid levels. Our research showed that AZ demonstrated elevated levels of PDH activity, PDK4, and downstream p-PDH/PDH expressions. This suggests that the lactate feedback mechanism induced by AZ-mediated PDK4 overexpression may trigger M2 macrophage polarization to repair inflammatory tissue damage caused by M1 macrophages. Notably, CPAZ also demonstrated CP-like effects, including decreased levels of PDH activity, PDK4, and downstream p-PDH/PDH expressions, though with slightly reduced impact compared to CP. This emphasized CP's primary role as a monarch drug in HGD. The compatibility of CP and AZ maintained balanced PDK4 expression, preventing excessive fluctuations, which may be essential for M1/M2 macrophage polarization equilibrium.

To establish whether PDK4 functions as the target of CP-induced inhibition of M1 macrophage polarization, a PDK4 overexpression mouse model was developed using AAV-PDK4. The results showed that AAV-PDK4 counteracted both the therapeutic effect and M1 macrophage polarization suppression of CP in colitis mice, demonstrating that M1 macrophage polarization reduction depends on CP-downregulated PDK4 and subsequent TCA cycle restoration. Furthermore, the PDK4/p-PDH signaling pathway was inhibited by PDK4 antagonist DCA to assess PDK4's role in AZ-induced enhancement of M2 macrophage polarization. The findings indicated that AZ-induced promotion of M2 macrophage polarization alleviation and improvement of colitis-associated symptoms were partially neutralized in the presence of DCA, highlighting the essential role of the PDK4/lactate axis in AZ-primed M2 macrophage polarization.

5. Conclusions

Taken together, compatibility of CP and AZ in HGD synergistically alleviated colitis mice through M1/M2 macrophage polarization balance *via* PDK4-mediated glucose metabolism reprogramming. Specifically, CP reduced M1 macrophage polarization by recovery of TCA cycle *via* PDK4 inhibition. AZ increased M2 macrophage polarization through activation of PDK4/lactate axis (Fig. 8). This study elucidates the scientificity and rationality of compatibility of CP and AZ, and offers experimental guidance for the future clinical application.

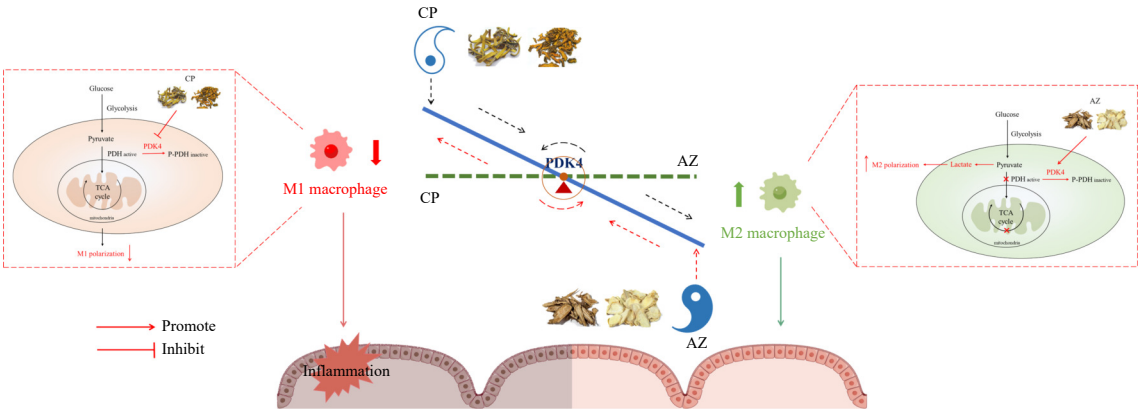

Fig. 8 Compatibility mechanism of CP and AZ regulated M1/M2 macrophage polarization.

Funding

This work was supported by the National Natural Science Foundation of China (Nos. 82374325 and 82074322) and GDAS' Project of Science and Technology Development (No. 2022GDASZH-2022010110).

Supplementary materials

Supplementary materials associated with this article can be requested by sending an E-mail to the corresponding authors.

Declaration of competing interest

All authors declare no conflict of interest.

References

1 Kobayashi T, Siegmund B, Le B, et al. Ulcerative colitis. *Nat Rev Dis Primers*. 2020;6(1):74. https://doi.org/10.1038/s41572-020-0205-x.
2 Kaluzna A, Olczyk P, Komosinska K. The role of innate and adaptive immune cells in the pathogenesis and development of the inflammatory response in ulcerative colitis. *J Clin Med*. 2022;11(2):400. https://doi.org/10.3390/jcm11020400.
3 Ahmad H, Kumar VL. Pharmacotherapy of ulcerative colitis--current status and emerging trends. *J Basic Clin Physiol Pharmacol*. 2018;29(6):581-592. https://doi.org/10.1515/jbcpp-2016-0014.
4 Harbord M, Eliakim R, Bettenworth D, et al. Third european evidence-based consensus on diagnosis and management of ulcerative colitis. Part 2: current management. *J Crohns Colitis*. 2017;11(7):769-784. https://doi.org/10.1093/ecco-jcc/jjx009.
5 Mas E, Calvo X. Selecting the best combined biological therapy for refractory inflammatory bowel disease patients. *J Clin Med*. 2022;11(4):1076. https://doi.org/10.3390/jcm11041076.
6 Na Y, Stakenborg M, Seok S, et al. Macrophages in intestinal inflammation and resolution: a potential therapeutic target in IBD. *Nat Rev Gastroenterol Hepatol*. 2019;16(9):531-543. https://doi.org/10.1038/s41575-019-0172-4.
7 Zhu W, Yu J, Nle Y, et al. Disequilibrium of M1 and M2 macrophages

correlates with the development of experimental inflammatory bowel diseases. *Immunol Invest*. 2014;43(7):638-652. https://doi.org/10.3109/08820139.2014.909456.
8 Hou X, Zhang L, Han L, et al. Differing roles of pyruvate dehydrogenase kinases during mouse oocyte maturation. *J Cell Sci*. 2015;128(13):2319-2329. https://doi.org/10.1242/jcs.167049.
9 Lee H, Jeon JH, Lee Y, et al. Inhibition of pyruvate dehydrogenase kinase 4 in $CD4^+$ T cells ameliorates intestinal inflammation. *Cell Mol Gastroenterol Hepatol*. 2023;15(2):439-461. https://doi.org/10.1016/j.jcmgh.2022.09.016.
10 Zou X, Liu D, Ding M, et al. Clinical effects of TCM syndrome differentiation and treatment on sixty-cases with ulcerative colitis. *Henan Tradit Chin Med*. 2015;35(7):1628-1630. https://doi.org/10.16367/j.issn.1003-5028.2015.07.0686.
11 Du B, Xu Z. Wumei pill combined with traditional Chinese medicine enema for treatment of cold and hot miscellaneous ulcerative colitis. *World J Integr Tradit West Med*. 2020;15(11):2098-2101. https://doi.org/10.13935/j.cnki.sjzx.201128.
12 Wu Q, Zhang S, Wang R, et al. Discussion in invaluable prescriptions for ready reference for recurrent dysentery from cold-heat syndrome. *China J Tradit Chin Med Pharm*. 2020;35(11):5427-5430.
13 Xie Q, Li H, Ma R, et al. Effect of *Coptis chinensis* Franch and *Magnolia officinalis* on intestinal flora and intestinal barrier in a TNBS-induced ulcerative colitis rats model. *Phytomedicine*. 2022;97:153927. https://doi.org/10.1016/j.phymed.2022.153927.
14 He Y, Li Y, Wu Y, et al. Huanglian Ganjiang decoction alleviates ulcerative colitis by restoring gut barrier *via* APOC1-JNK/P38 MAPK signal pathway based on proteomic analysis. *J Ethnopharmacol*. 2024;318(Pt B):116994. https://doi.org/10.1016/j.jep.2023.116994.
15 Li Y, He Y, Wu Y, et al. Compatibility between cold-natured medicine CP and hot-natured medicine AZ synergistically mitigates colitis mice through attenuating inflammation and restoring gut barrier. *J Ethnopharmacol*. 2023;303:115902. https://doi.org/10.1016/j.jep.2022.115902.
16 Li Y, Wang X, Su Y, et al. Baicalein ameliorates ulcerative colitis by improving intestinal epithelial barrier *via* AhR/IL-22 pathway in ILC3s. *Acta Pharmacol Sin*. 2022;43(6):1495-1507. https://doi.org/10.1038/s41401-021-00781-7.
17 Zhuang H, Lv Q, Zhong C, et al. Tiliroside ameliorates ulcerative colitis by restoring the M1/M2 macrophage balance *via* the HIF-1α/glycolysis pathway. *Front Immunol*. 2021;12:649463. https://doi.org/10.3389/fimmu.2021.649463.
18 Weisser S, Van R, Sly L. Depletion and reconstitution of macrophages in mice. *Jove-J Vis Exp*. 2012;(66):4105. https://doi.org/10.3791/4105.
19 Phan K, Ng W, Lu V, et al. Association between IDH1 and IDH2 mutations and preoperative seizures in patients with low-grade versus high-grade glioma: a systematic review and meta-analysis. *World Neurosurg*. 2018;111:E539-E545. https://doi.org/10.1016/j.wneu.2017.12.112.
20 Panaccione R, Ghosh S, Middleton S, et al. Combination therapy with infliximab and azathioprine is superior to monotherapy with either agent in ulcerative colitis. *Gastroenterology*. 2014;146(2):392-400. https://doi.org/10.1053/j.gastro.2013.10.052.
21 Ji S, He D, Su Z, et al. P450 enzymes-based metabolic interactions between monarch drugs and the other constituent herbs: a strategy to explore compatibility mechanism of Sangju-Yin. *Phytomedicine*. 2019;58:152866. https://doi.org/10.1016/j.phymed.2019.152866.
22 Wang S, Hu Y, Tan W. et al. Compatibility art of traditional Chinese medicine: from the perspective of herb pairs. *J Ethnopharmacol*. 2012;143(2):412-423. https://doi.org/10.1016/j.jep.2012.07.033.
23 Yang Z, Lin S, Feng W, et al. A potential therapeutic target in traditional Chinese medicine for ulcerative colitis: macrophage polarization. *Front Pharmacol*. 2022;13:999179. https://doi.org/10.3389/fphar.2022.999179.
24 Kim M, Lee H, Chanda D. et al. The role of pyruvate metabolism in mitochondrial quality control and inflammation. *Mol Cells*. 2023;46(5):259-267. https://doi.org/10.14348/molcells.2023.2128.
25 Angajala A, Lim S, Phillips J, et al. Diverse roles of mitochondria in immune responses: novel insights into immuno-metabolism. *Front Immunol*. 2018;9:1605. https://doi.org/10.3389/fimmu.2018.01605.
26 Infantino V, Convertini P, Cucci L, et al. The mitochondrial citrate carrier: a new player in inflammation. *Biochem J*. 2011;438:433-436. https://doi.org/10.1042/BJ20111275.
27 Everts B, Amiel E, Huang S, et al. TLR-driven early glycolytic reprogramming *via* the kinases TBK1-IKKε supports the anabolic demands of dendritic cell activation. *Nature Immunol*. 2014;15(4):323-332. https://doi.org/10.1038/ni.2833.
28 Infantino V, Iacobazzi V, Palmieri F, et al. ATP-citrate lyase is essential for macrophage inflammatory response. *Biochem Biophys Res Commun*. 2013;440(1):105-111. https://doi.org/10.1016/j.bbrc.2013.09.037.
29 Liu P, Wang H, Li X, et al. α-Ketoglutarate orchestrates macrophage activation through metabolic and epigenetic reprogramming. *Nature Immunol*. 2017;18(9):985-994. https://doi.org/10.1038/ni.3796.
30 Tannahill G, Curtis A, Adamik J, et al. Succinate is an inflammatory signal that induces IL-1β through HIF-1α. *Nature*. 2013;496(7444):238-242. https://doi.org/10.1038/nature11986.
31 Wang F, Wang K, Xu W, et al. SIRT5 desuccinylates and activates pyruvate kinase M2 to block macrophage IL-1β production and to prevent DSS-induced colitis in mice. *Cell Rep*. 2017;19(11):2331-2344. https://doi.org/10.1016/j.celrep.2017.05.065.
32 Ivashkiv L. The hypoxia-lactate axis tempers inflammation. *Nat Rev Immunol*. 2020;20(2):85-86. https://doi.org/10.1038/s41577-019-0259-8.
33 Mu X, Shi W, Xu Y, et al. Tumor-derived lactate induces M2 macrophage polarization *via* the activation of the ERK/STAT3 signaling pathway in breast cancer. *Cell Cycle*. 2018;17(4):428-438. https://doi.org/10.1080/15384101.2018.1444305.
34 Locatelli S, Careddu G, Serio S, et al. Targeting cancer cells and tumor microenvironment in preclinical and clinical models of hodgkin lymphoma using the dual PI3Kδ/γ inhibitor RP6530. *Clin Cancer Res*. 2019;25(3):1098-1112. https://doi.org/10.1158/1078-0432.CCR-18-1133.
35 Liu N, Luo J, Kuang D, et al. Lactate inhibits ATP6V0d2 expression in tumor-associated macrophages to promote HIF-2α-mediated tumor progression. *J Clin Invest*. 2019;129(2):631-646. https://doi.org/10.1172/JCI123027.
36 Zhou H, Yan X, Yu W, et al. Lactic acid in macrophage polarization: the significant role in inflammation and cancer. *Int Rev Immunol*. 2022;41(1):4-18. https://doi.org/10.1080/08830185.2021.1955876.
37 Zhang D, Tang Z, Huang H, et al. Metabolic regulation of gene expression by histone lactylation. *Nature*. 2019;575-580(7779):575-580. https://doi.org/10.1038/s41586-019-1678-1.
38 Chen Y, Wu G, Li M, et al. LDHA-mediated metabolic reprogramming promoted cardiomyocyte proliferation by alleviating ROS and inducing M2 macrophage polarization. *Redox Biol*. 2022;56:102446. https://doi.org/10.1016/j.redox.2022.102446.
39 Zhou H, Yu W, Yan X, et al. Lactate-driven macrophage polarization in the inflammatory microenvironment alleviates intestinal inflammation. *Front Immunol*. 2022;13:1013686. https://doi.org/10.3389/fimmu.2022.1013686.
40 Gao Y, Zhou H, Liu G, et al. Tumor microenvironment: lactic acid promotes tumor development. *J Immunol Res*. 2022;2022:3119375. https://doi.org/10.1155/2022/3119375.
41 Adam C, Paolini L, Gueguen N, et al. Acetoacetate protects macrophages from lactic acidosis-induced mitochondrial dysfunction by metabolic reprograming. *Nat Commun*. 2021;12(1):7115. https://doi.org/10.1038/s41467-021-27426-x.
42 Pålsson-mcdermott E, O'neill L. Targeting immunometabolism as an anti-inflammatory strategy. *Cell Res*. 2020;30(4):300-314. https://doi.org/10.1038/s41422-020-0291-z.
43 Woolbright B, Rajendran G, Harris R, et al. Metabolic flexibility in cancer: targeting the pyruvate dehydrogenase kinase: pyruvate dehydrogenase axis. *Mol Cancer Ther*. 2019;18(10):1673-1681. https://doi.org/10.1158/1535-7163.MCT-19-0079.